Available online at www.sciencedirect.com
ScienceDirect
Thin Solid Films 516 (2008) 8399–8407
www.elsevier.com/locate/tsf

Preparation and properties of nano-silica modified negative acrylate photoresist

Chih-Kang Lee, Trong-Ming Don, Wei-Chi Lai, Chin-Chung Chen, Dar-Jong Lin, Liao-Ping Cheng *

Department of Chemical and Materials Engineering, Tamkang University, Taipei, 25137, Taiwan

Received 30 May 2007; received in revised form 25 February 2008; accepted 7 April 2008
Available online 12 April 2008

Abstract

A series of silica modified photoresists had been successfully developed through incorporation of a particular nanoparticles suspension. Free radical polymerization was employed to synthesize the binder, an acrylate copolymer resin of benzyl methacrylate, methacrylic acid and 2-hydroxyethyl methacrylate, of the photoresist. The acid value, viscosity, molecular weight and thermal properties of the formed binders were measured. Then, surface-modified silica particles prepared by the sol–gel method were introduced to the photoresist. Because the modified silica particles contained considerable amount of reactive double bonds (C═C) on their surfaces, they would react with the polyfunctional monomers in the photoresist to form an organic–inorganic nanohybrid. Fourier transform infrared spectrometer was used to analyze the evolution of chemical bonds at various stages of the preparation process. Thermal analyses including thermal gravimetric analyzer, differential scanning calorimeter and thermo-mechanical analyzer were used to evaluate the level of enhancement on thermal and dimensional stabilities of the photoresist due to silica incorporation.
© 2008 Elsevier B.V. All rights reserved.

Keywords: Photoresist; Binder; Sol–gel method; Organic–inorganic nanohybrid

1. Introduction

Photoresists are widely used for the manufacture of microelectronics, silk screen printings, printed circuit boards, optical disks, color filter resists and so on. The recipe of a common negative-type photoresist consists of a binder, photosensitive polyfunctional monomer, photoinitiator, solvents and pigments [1–5]. For a photoresist applied in color filter, the binder plays a vital role, as it determines the adhesion strength, hardness, heat resistance, and developability of the photoresist [6]. In this research, a series of binders was synthesized from free radical copolymerization of three kinds of acrylate monomers benzyl methacrylate (BZMA), methacrylic acid (MAA), and 2-hydroxyethyl methacrylate (2-HEMA). The synthetic route of these binders is outlined in Scheme 1. The thermal behaviors, molecular weights, and acid values of the prepared binders were measured and compared so as to optimize the thermal mechanical and chemical stability properties of the photoresist.

Organic–inorganic hybrid materials have been extensively investigated in recent years [7–13]. Organic polymers, as characterized by good flexibility, ductility and processability, have long been applied in various industries. In contrast, inorganic materials possess properties, such as high rigidity, mechanical strength, and thermal stability that are not achievable by polymers. Combination of the advantages of these two classes of materials to yield a composite with superior properties that meet the industrial standards is nowadays highly demanded. To prepare such organic–inorganic hybrid materials, a modified sol–gel process is generally used. Sol–gel process was originally developed for the low-temperature synthesis of glass or ceramic materials, which involves consecutive hydrolysis and condensation of an alkoxysilane to form silicone oxide particles that suspend in an aqueous/alcoholic solution; e.g., silica can be formed from hydrolysis and condensation of tetraethoxysilane (TEOS). The related theories are built upon colloidal science, and the basic principles can be found in

* Corresponding author. Tel.: +886 2 26215656x2614 or 2725; fax: +886 2 26209887.
E-mail address: lpcheng@mail.tku.edu.tw (L.-P. Cheng).

0040-6090/$ - see front matter © 2008 Elsevier B.V. All rights reserved.
doi:10.1016/j.tsf.2008.04.051

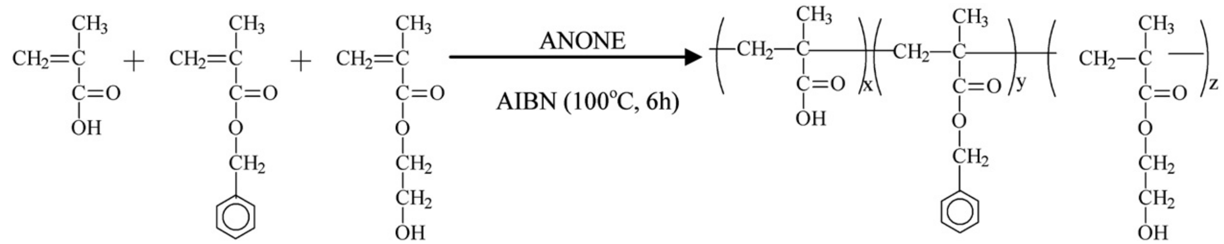

Scheme 1. Preparation of poly(BZMA–MAA–2-HEMA) by free radical polymerization.

previous literature [14,15]. Furthermore, the composite material is optically transparent, and is therefore suited to optoelectronic applications [16–18].

In this research, a nano-silica modified photoresist was developed by introduction through covalent bonding of surfaced-modified silica particles into the polymer matrix of the photoresist. The modified silica particles contained considerable amount of reactive double bonds (C═C) on their surfaces, which would react with the polyfunctional monomers in the photoresist to form an organic–inorganic hybrid during the UV-curing step for photoresist processing. The route for the synthesis of surface-modified silica particles is outlined in Scheme 2. Tsushima et al. [19] demonstrated that the photoresist consisting of polysilane and silica gel exhibited higher heat resistance than those without using silica. Silian type coupling agents used for improving the adhesion and hardness on glass substrate were reported in the literature [4]. In the case of conventional acrylic photoresist applied in color filter, the required resolution and heat stability were 10 ~ 20 µm and 220 ~ 300 °C, as was reported by Sabnis et al. [6]. The organic–inorganic hybrid photoresist developed in the present work demonstrated improved mechanical strength, thermal and dimensional stability compared with conventional organic-based photoresists, while holding the resolution <10 µm. The resolution, heat resistance, hardness, and adhesion meet the industrial standards of photoresists applied in color filters.

2. Experimental details

2.1. Materials

Materials for the preparation of poly(acrylate)/SiO_2 nanoparticles photoresist includes BZMA, MAA, 2-HEMA, 2,2′-azobisisobutyronitrile (AIBN), 1-dodecanethiol

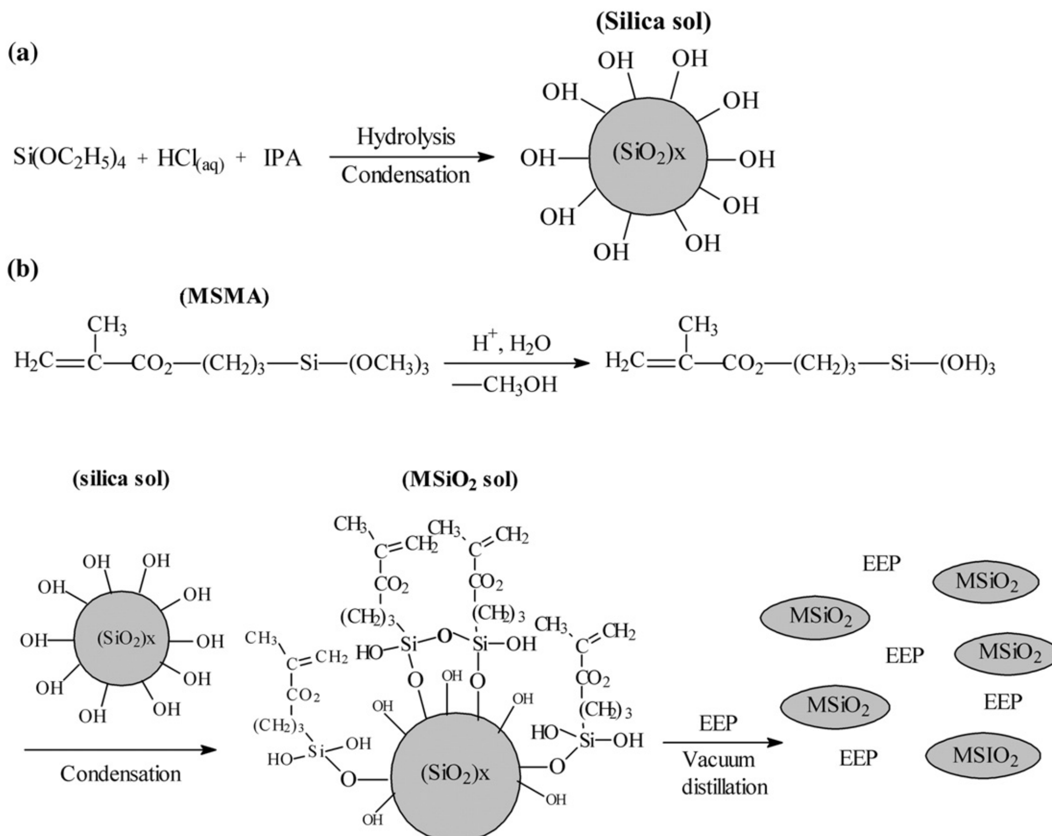

Scheme 2. Preparation of silica sol (a) and $MSiO_2$ nanoparticles suspension (b) by hydrolysis and condensation from TEOS and MSMA.

(Thiol), tetraethoxylsilane (TEOS), 3-(trimethoxysilyl) propyl methacrylate (MSMA), 2-propanol (IPA), ethyl 3-ethoxypropionate (EEP), cyclohexanone (ANONE), propylene glycol methyl ether acetate (PMA), and dipentaerythritol hexaacrylate (DPHA). All of them are reagent grade and purchased from Aldrich Chemical Co., USA. Photoinitiators, α-aminoketone (Irgacure 369) and isopropyl thioxanthone (ITX), were supplied by Ciba-Geigy Ltd. All materials were used as received.

2.2. Preparation of binders

The solutions of binder were prepared by free radical copolymerization of three kinds of acrylate monomers BZMA, MAA, and/or 2-HEMA in cyclohexanone (cf., Scheme 1; solid content = 40 wt.%). Appropriate amounts of the monomers were dissolved in the solvent; the compositions are shown in Table 1. The solution was preheated at 100 °C and stirred under nitrogen atmosphere. The initiator (AIBN, 1 wt.% of monomers) and chain-transfer agent (Thiol, 1 wt.% of monomers) were also dissolved in the same solvent before dropping into the monomer solution. The free radical polymerization was carried out for 6 h, and then the product was cooled to room temperature. The obtained acrylate resin, i.e., poly(BZMA–MAA–2-HEMA) dissolved in cyclohexanone, was used as the binder of the photoresist. To prepare samples for thermal property measurements and chemical structure identifications, the binder solution was diluted with tetrahydrofuran (THF) and then poured into hexane to induce polymer precipitation. The precipitation procedure was repeated twice to ensure free of residual monomers. Finally, the polymeric white-powders were separated by filtration and were dried in vacuo at 60 °C. The compositions for various binders are listed in Table 1.

2.3. Preparation of $MSiO_2$ nanoparticles suspension and photoresists

The silica sol was prepared by hydrolysis and condensation of TEOS in IPA at room temperature. The molar ratio of IPA/TEOS was 1.1, and hydrochloric acid aqueous solution at pH 1.3 was used as a catalyst. The reactants were stirred for 3 h, and then the coupling agent, MSMA, with molar ratio of TEOS/MSMA = 4.5, was dropped into the silica sol. After reaction for another 3 h, surface-modified silica (called $MSiO_2$) sol was obtained. To remove the residual by products (e.g., ethanol, methanol, IPA, water and HCl), the prepared $MSiO_2$ sol was mixed with EEP, used as a dispersant for $MSiO_2$ nanoparticles. After vacuum distilled at 30 °C for 1 h, a transparent $MSiO_2$ suspension was obtained (cf., Scheme 2).

Subsequently, a negative photoresist was prepared by adding appropriate amounts of $MSiO_2$ nanoparticles suspension to the conventional polymeric-photoresist. The organic–inorganic hybrid photoresist was composed of binder (8 wt.%), polyfunctional monomer DPHA (8 wt.%), photoinitiator and photosensitizer (0.6 wt.%, Irgacure 369/ITX = 5), and various ratios of $MSiO_2$ suspension (5–20 wt.% of the organic moiety of photoresist) mixed in a tri-solvent. The final composition of the tri-solvent was adjusted to ANONE/EEP/PMA = 0.87/1/1 in molar ratio. The viscosity of photoresist could be adjusted by the amount of tri-solvent to give a satisfactory coatability.

2.4. Characterization

Several methods were adopted to characterize the binders and the photoresists:

1. Gel permeation chromatography (GPC, Waters 1515 Isocratic HPLC Pump) was performed with THF as the mobile phase at 40 °C with a polystyrene gel column (AM GPC Gel). Molecular weights of the binders are reported based on polystyrene standards.
2. Infrared absorption spectra of the binder and $MSiO_2$ sols were taken using a Fourier transform infrared spectrophotometer (Nicolet spectrometer 550, USA). Powders of binder were ground with KBr to form a disc (1: 50) for FTIR scanning. Both silica and $MSiO_2$ samples were prepared by dropping appropriate amounts of the sols onto a KBr disc, and then the solvent was evaporated at 80 °C for 10 min. For all scans, the spectra were collected over the wavenumber range of 400–4000 cm^{-1} with a resolution of 4 cm^{-1}.
3. Acid values of the prepared binders were determined by titration using a 0.1 mol/dm^3 potassium hydroxide (KOH) solution. The definition of acid value is the amount of KOH in milligrams needed to reach the equivalent point for 1 g of the prepared binder (mg/g).
4. Thermal gravimetric analyzer (TGA), Hi-Res TGA 2950 from TA instruments Ltd., USA, was used to measure the thermal decomposition temperature (T_d) of the binder and the cured films of the photoresists. Samples (8–12 mg) were heated from room temperature to 600 °C with a heating rate of 10 °/min under nitrogen flow.

Table 1
Compositions and properties of the synthesized binders

Binder code	Composition (mol%)			Average molecular weight (M_w)	PDI	Thermal properties		Acid value [a]
	BZMA	MAA	2-HEMA			T_g (°C)	T_d (°C)	
B80M20H0	80	20	0	2.30×10^4	1.19	87.6	331.6	76.2
B72M18H10	72	18	10	2.19×10^4	1.23	87.1	328.8	70.2
B64M16H20	64	16	20	2.16×10^4	1.20	86.5	314.4	63.3
B56M14H30	56	14	30	2.05×10^4	1.18	86.2	307.9	58.1
B63M27H10	63	27	10	2.11×10^4	1.16	99.9	329.7	108.1
B54M36H10	54	36	10	1.99×10^4	1.16	120.4	329.8	152.3

[a] Milligrams of KOH/g of binder polymer.

5. Differential scanning calorimeter (DSC) was employed to measure the glass transition temperature (T_g) of the binder and the films of photoresist. DSC, model 2010, TA Instrument Ltd., USA, was first calibrated with indium standard before running the tests. An appropriate amount of a dried sample was sealed in an aluminum pan and placed in the heating chamber together with an empty reference pan. The temperature was raised from 50 °C to 170 °C at a constant rate of 20 °C/min under nitrogen flow. T_g of the sample was determined from the thermogram of the second heating cycle.
6. The particle size of $MSiO_2$ was obtained from the dynamic light scattering measurement using a Zetasizer (Malvern, DTS 1060) at 25 °C. The instrument was equipped with a monochromatic coherent helium neon laser (633 nm) as the light source. A 4 ml $MSiO_2$ sol solution was injected into the quartz cuvette and the scattered light was recorded at an angle of 90°.
7. The thermal dimensional stability of the prepared films was studied with a thermo-mechanical analyzer, TMA, model TMA Q400 from TA instruments Ltd., USA. The coefficients of thermal expansion (CTE), α_1 and α_2, were obtained by measuring the linear dimensional variations (ΔL) at different temperatures. The T_g of a sample was identified as the intercept of the two tangent lines where a change in slope occurred, i.e., above and below T_g. Samples (4 × 8 mm) were heated from 30 °C to 180 °C with a heating rate of 10 °C/min in a nitrogen atmosphere.
8. Tape test, also called peel test, was carried out to evaluate the adhesion of the films coated on a glass substrate. The degree of adhesion between the film and the glass substrate increases as the percentage of the residual film on the glass after the tape test [20]. The hardness of the formed films was examined by the industrial pencil hardness test with pencils of different hardness [21].
9. Resolution of the negative-type photoresist was determined by examining the developed circuit diagram under microscope. The exposure-development procedure was as follows:

a) The negative-type photoresist was uniformly spread on a glass substrate using a spin-coator (1500 rpm), and then prebaked at 80 °C for 5 min.
b) Following UV irradiation under a photomask at 250 mJ/cm^2 (UV source: broadband, 235–400 nm, local maxima at 257, 313, and 365 nm, Group Up Ind. Co., Japan), it was then developed with a developer liquid, IPA/H2O/Na2CO3 = 3/2/0.02.
c) Before using optical microscope to examine the resolution, the photoresist was postbaked at 200 °C for 1 h to obtain a cured coating (about 1–2 µm in thickness).

3. Results and discussion

3.1. Characterization of binders

3.1.1. Molecular weight measurements

In this study, AIBN was used as initiator and Thiol was used as chain-transfer agent for binder synthesis. They contributed not only to control the molecular weight of the synthesized copolymer but also to give a binder with relatively narrow polydispersity [22]. If the molecular weight of the prepared binder was too small, the developability of the photoresist would be excessively rapid. This made it difficult to control pattern shape during the development process. Even if patterns could be formed, problems such as a reduction of final coating thickness could occur. On the contrary, as the molecular weight of the binder was too large, the viscosity of the photoresist solution was too high and this could affect the coatability. Furthermore, the developability might also be deteriorated making it difficult to form sharp patterns [1]. The weight average molecular weight (M_w) and polydispersity index (PDI) values of the prepared binders was measured using GPC, as listed in Table 1. M_w of all prepared binders was found to be ranging from 2.0×10^4 to 2.3×10^4 g/mole, and PDI from 1.16 to 1.23. It indicates that both AIBN and thiol contents restricted to 1 wt.% of monomers were reasonable in the present synthesis process.

3.1.2. Thermal properties

3.1.2.1. Glass transition temperature. Glass transition temperatures (T_g) of pure poly(benzyl methacrylate), poly(2-hydroxyethyl methacrylate) and poly(methacrylic acid) are 54, 55 and 166 °C, respectively, as obtained from the literature [23,24]. Attempts have been made to measure T_g of the prepared binders by means of DSC. The thermograms of the prepared binders are shown in Fig. 1. It appears that T_g of the binders from B80M20H0 to B56M14H30 (BZMA/MAA = 4, molar ratio) were very close and ranged from 86 to 88 °C, as indicated in Table 1. The values were very close even when the 2-HEMA content was 30 mol%. However, T_g of the B80M20H0 still slightly higher than that of B56M14H30, ca. 1.4 °C, due to the higher content of MAA. On the other hand, as 2-HEMA content was limited to 10 mol%, e.g., B72M18H10, B63M27H10 and B54M36H10, T_g increased obviously with increasing MAA content, in accordance with the results from literature [25].

3.1.2.2. Thermal degradation. TGA was utilized to measure the thermal decomposition behaviors of various binders. Fig. 2

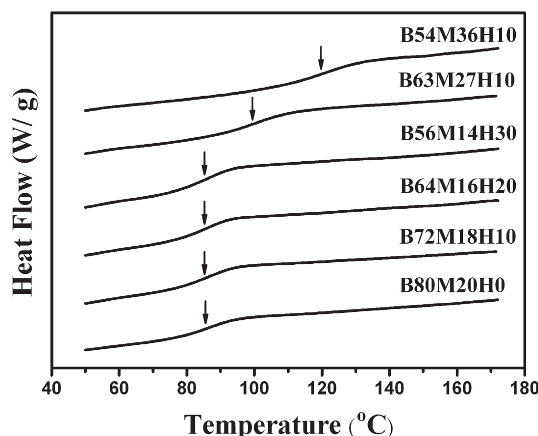

Fig. 1. DSC thermograms of the prepared binders.

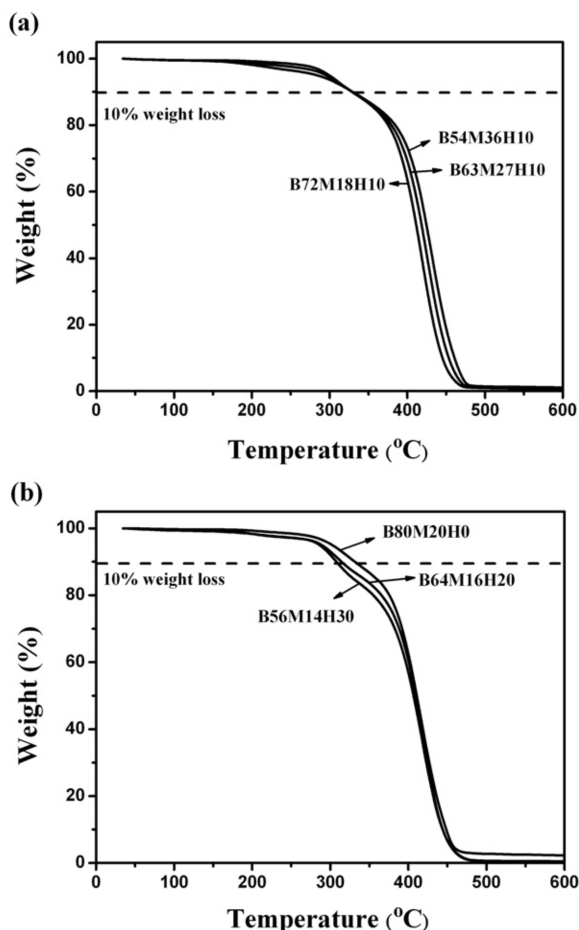

Fig. 2. TGA thermograms of the prepared binder polymers. (a) 2-HEMA content is10 mol%; (b) molar ratio of BZMA/MAA is 4.

shows TGA thermograms of the prepared binders, in which thermal decomposition of the prepared binders generally follows a three-stage pattern. For all binders, the first, second and the third stage decompositions occurred at about 180–270 °C, 270–370 °C and 370–470 °C, respectively. The weight loss in the first stage could be attributed to the reactions of MAA with adjacent MAA or 2-HEMA monomer unit, for which water was lost from the formation of anhydride or ester group, as pointed out by Mansur et al. [23,25]. Because the ranges of thermal decompositions of poly(2-HEMA) and poly(BZMA) were 290–400 °C and 270–370 °C, respectively, the second stage decomposition was attributed to both 2-HEMA and BZMA segments. Therefore, the weight loss of the binder containing 72% BZMA, B72M18H10, in Fig. 2(a) was most serious over the temperature range of 270–370 °C. For the third stage decomposition, the weight loss could largely be attributed to the MAA units (the thermal decomposition range of poly(MAA) is 370–470 °C) in the prepared binders. It was found that the third stage degradation temperature increased as the MAA content increased. This is probably due to the increasing content of anhydride groups formed in the first stage of degradation. Fig. 2 (a) demonstrates that the binder B54M36H10, MAA content = 36%, has the most weight loss of the first stage and the highest degradation temperature of the third stage. Fig. 2(b) shows that the extent of the first stage decomposition increased as the total amount of both 2-HEMA and MAA content increased (dehydration reaction); furthermore, the decomposition extent of the binder "B56M14H30" was the highest over the temperature range of 290–400 °C due to its high 2-HEMA content. Because thermal decomposition behaviors of the prepared binders were complicate and involved three stages, the temperature corresponding to 10 wt.% loss was identified as the thermal degradation temperature, T_d, for easy comparison. The results are listed in Table 3.

3.1.3. Chemical structure characterization

Fig. 3(a) illustrates the FTIR spectrum of the prepared binder, B54M36H10. The absorption peaks at 3500 and 3261 cm^{-1} were due to the –OH stretching band of hydroxyl group and carboxyl group, respectively. The =C−H stretching band of the aromatic ring (BZMA unit) was observed from 2950 to 3065 cm^{-1}, and the C=O stretching band of the carbonyl group at 1729 cm^{-1} (MAA unit) and 1708 cm^{-1} (2-HEMA unit) could also be observed. For the 2-HEMA unit, the stretching band of the ester group (C−O−C) was observed at 1146 cm^{-1}. Furthermore, two C−H vibration bands of monosubstituted benzene (BZMA unit) were observed at 701 and 748 cm^{-1}. The spectrum suggests that the three kinds of acrylate monomers were linked together to form a binder in the free radical polymerization. Fig. 3(b) shows FTIR spectrum of the binder, B54M36H10, that was baked at 220 °C for 1 h. The asymmetric and symmetric stretching vibrations of the two C=O groups of a formed anhydride were observed at 1805 cm^{-1} and 1762 cm^{-1}, respectively; furthermore, the acid anhydride also has a strong band at 1019 cm^{-1} due to the C−O−C stretching vibration. This result indicates that the anhydride was produced after the binder was baked at 220 °C for 1 h. That is, as the binder contains more MAA or 2-HEMA, the weight loss in the first-stage degradation of TGA experiment would be more pronounced, in accordance with the TGA result shown in Fig. 2(a).

3.1.4. Acid value measurement

The carboxyl groups of the binder provide acid value in a negative-type photoresist. If the acid value of the binder is too small, the solubility of the prebaked photoresist in an alkaline

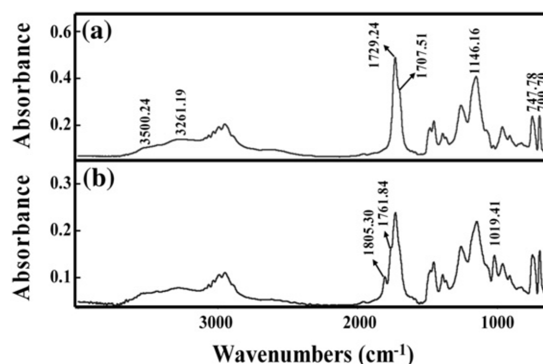

Fig. 3. FTIR spectra of the binder, B54M36H10. (a) before; (b) after baked at 220 °C for 1 h.

developer liquid will be too low, which causes an excess amount of development residue, i.e., poor developability. Also, poor adhesion to the substrate may occur when the acid value is too low. On the other hand, when the acid value is too large, the film may dissolve too much in the developer liquid [26]. Acid values of the prepared binders are shown in Table 1. As expected, the acid value increases as the MAA content increases. That is, the solubility of a binder in an alkaline developer liquid is directly related to the MAA content of the binder. Based on the thermal properties and the acid values, the binders, B63M27H10 and B54M36H10, were chosen to prepare the nano-silica modified photoresists in the subsequent experimental process, and the formed photoresists were termed PR63 and PR54 series, respectively, in the discussion that follows.

3.2. Modification of silica nanoparticles

3.2.1. Characterization

Evolution of chemical bonds during the sol–gel process shown in Scheme 2 was analyzed using FTIR. In Fig. 4, the spectra of $MSiO_2$ and silica sols obtained by a sol–gel process are demonstrated. For the silica sol, cf. Fig. 4(a), the adsorption bands at 1073 and 797 cm^{-1} represent the asymmetric and symmetric stretching vibrations of the Si−O−Si bond, respectively. The 454 cm^{-1} band is the bending vibration of this bond. The bands for −Si−O−C− and Si−OH stretching vibrations are located at 1163 cm^{-1} and 3326 cm^{-1}, respectively. The adsorption band at 945 cm^{-1} is assigned to the Si−OH bond [27]. From examination of the spectrum of $MSiO_2$ sol in Fig. 4(b), condensation reaction between MSMA and silica to produce $MSiO_2$ nanoparticles can be confirmed. The first feature comes from the Si−OH absorption band of $MSiO_2$ sol at 945 cm^{-1}. Its intensity is lower than silica sol in Fig. 4(a) due to the decrease of Si−OH groups content on the surface of silica particles. The second feature is the adsorption bands of C=C and C=O appearing at 1630 cm^{-1} and 1700 cm^{-1}, respectively. This indicates that after hydrolysis and condensation of MSMA with the silica sol, the modified nanoparticles contain considerable amount of reactive double bonds (C=C) on their surfaces, which can react with the polyfunctional monomer, DPHA, in the photoresist to form an organic–inorganic nanohybrid.

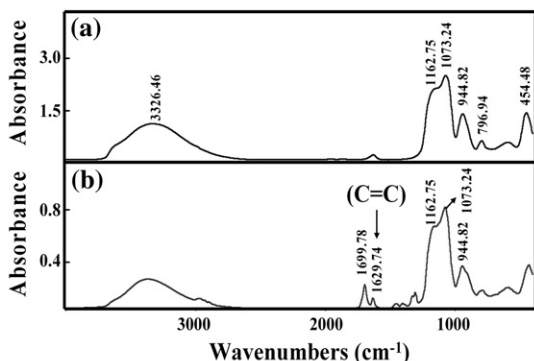

Fig. 4. FTIR spectra of (a) silica sol (b) $MSiO_2$ sol.

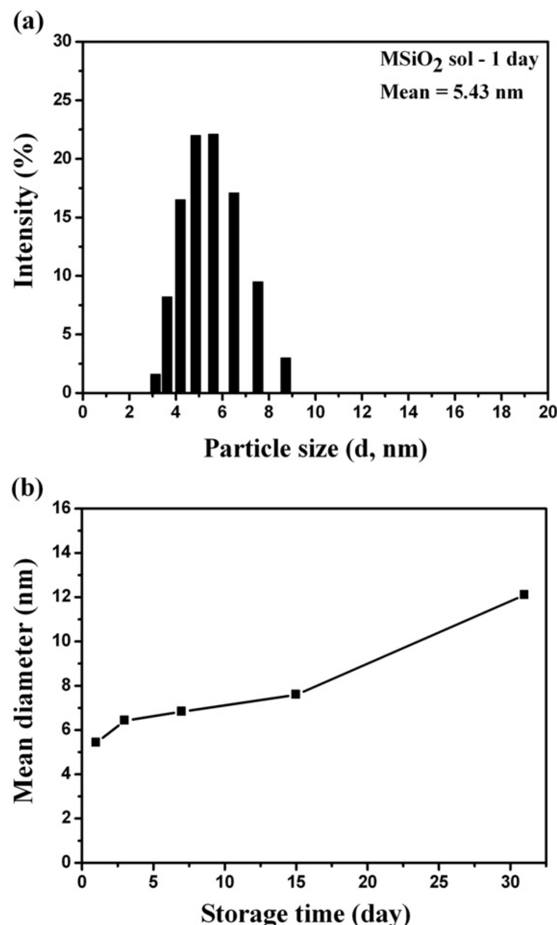

Fig. 5. Particle size analysis of the $MSiO_2$ sol stored at 4 °C for (a) 1 day and (b) 1–30 days.

3.2.2. Particle size

The modified $MSiO_2$ particles may grow and aggregate to become larger particles during the course of storage. Particle size of the prepared $MSiO_2$ sol measured at different storage time (1–30 days, stored at 4 °C) is shown in Fig. 5. It can be seen that the mean particle size of $MSiO_2$ sol was about 5–6 nm within 24 h in storage, cf. Fig. 5(a). As the storage time increased, the mean particle size of $MSiO_2$ increased as well; its final particle size was about 12 nm after 30 days. Fig. 5(b) reveals that the size of the $MSiO_2$ nanoparticles can be maintained smaller than 10 nm if the storage time is less than ca. 24 days.

3.3. Characterization of nano-silica modified photoresist

Photoresist generally consists of binder, polyfunctional monomer, photoinitiator, and photosensitizer. In this research the binders, B63M27H10 and B54M36H10, were selected to prepare the nano-silica modified photoresists. The formed photoresists with different compositions of $MSiO_2$ nanoparticles were termed the series “PR63-x” and “PR54-x”, and their compositions are listed in Table 2. After the photoresist was applied on the glass substrate, a cured film was obtained following the industrial process which included prebaking, UV exposure and postbaking. The nano-silica modified photoresist is expected

Table 2
Thermal properties of various photoresists

Sample name	$MSiO_2$ content (wt.%)	CTE (μm/m °C)		T_d (°C)	T_g (°C)	
		α_1	α_2		TMA	DSC
PR63	0	221.6	462.3	387.8	101.7	99.1
PR63-MSi5	5	194.7	371.6	388.2	103.6	100.3
PR63-MSi10	10	173.5	368.1	395.7	104.7	103.6
PR63-MSi15	15	164.3	291.4	396.5	108.6	104.9
PR63-MSi20	20	160.9	260.1	398.8	110.3	109.3
PR54	0	203.9	614.5	384.9	113.6	113.8
PR54-MSi5	5	197.3	561.9	389.1	114.8	116.7
PR54-MSi10	10	177.6	492.4	399.4	119.1	121.7
PR54-MSi15	15	163.9	325.8	402.4	121.6	122.9
PR54-MSi20	20	147.1	275.3	406.1	124.7	123.6

to exhibit improved hardness, adhesiveness, and thermal endurance with respect to conventional polymeric-photoresists.

3.3.1. Thermal properties

3.3.1.1. Glass transition temperature. The glass transition temperature of the cured films of nano-silica modified photoresist was determined by DSC, and the obtained thermograms of the series PR63-x and PR54-x are shown in Fig. 6. For the cured photoresists PR63 and PR54, free of $MSiO_2$ content, T_g are identified to be 99.1 and 113.8 °C, respectively. Note that T_g of the binder B54M36H10 is higher than that of B63M27H10, which implies that T_g of the photoresist depends on T_g of the binder. On the other hand, T_g of the nano-silica modified photoresists increased progressively with increasing $MSiO_2$ content, and when the $MSiO_2$ content reached 20 wt.%, T_g of the formed film can increase by 10 °C for both series of photoresists, as shown in Table 2. Thus, it can be concluded that T_g of the photoresists could be effectively increased either by using binder with a high T_g or $MSiO_2$ nanoparticles in the photoresist.

3.3.1.2. Thermal degradation. Thermal decomposition behaviors of the cured photoresists were investigated using TGA. The temperature corresponding to 10 wt.% loss was defined as the initial thermal degradation temperature. Fig. 7 shows the thermograms of the PR63-x and PR54-x series of nano-silica modified photoresists. It can be seen that all of the samples remain relatively stable against thermal decomposition even when the temperature was raised up to about 250 °C; the weight loss was smaller than 2%. Furthermore, T_d increased mildly with increasing $MSiO_2$ content for both series of samples, as summarized in Table 2. In the extreme case, PR54-MSi20, its initial thermal degradation temperature was ca. 21° higher than that of PR54 (cf. Fig. 7(b)). In addition, the char yield also increased with increasing inorganic nano-silica content, as expected [27].

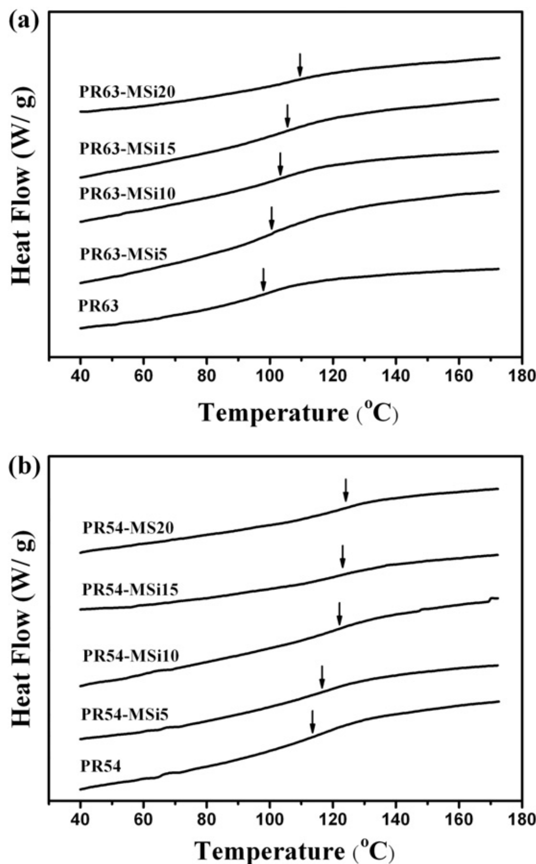

Fig. 6. DSC thermograms of the photoresists. (a) PR63-x; (b) PR54-x.

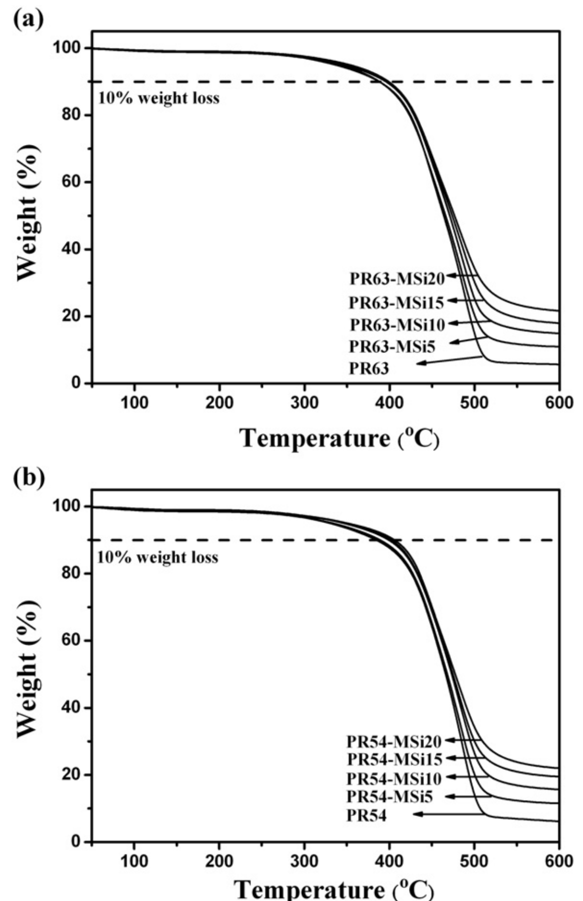

Fig. 7. TGA thermograms of the photoresists. (a) PR63-x; (b) PR54-x.

3.3.1.3. Thermal expansion coefficient. The linear thermal expansion coefficients (α) and T_g of various photoresists were measured using TMA and the results are shown in Fig. 8 and Table 2. As an example, Fig. 8 shows the thermograms of the cured photoresists, PR54 and PR54-MSi20, in terms of linear dimensional change versus temperature. For samples free of $MSiO_2$, Fig. 8(a) indicates that its thermal expansion coefficients before (α_1) and after (α_2) glass transition were 204 and 615 μm/m °C, respectively. T_g of this sample, as determined by the intersection of the two straight lines above and below the transition, was 114 °C, a value very close to the result measured using DSC. The thermal expansion coefficients of polymers are normally very high, and this limits their industrial applications as coating materials. This shortcoming can be overcome by incorporation of inorganic nano-silica into the polymer host. From Table 2, it can be seen that α_1 and α_2 of the formed photoresist films decreased with increasing nano-silica content. Specifically, α_1 and α_2 of the nano-silica modified photoresist "PR54-MSi20" were reduced to 147 and 275 μm/m °C, respectively (cf. Fig. 8(b)). In other words, the thermal dimensional stability of the sample has been enhanced due to the rigidity offered by $MSiO_2$.

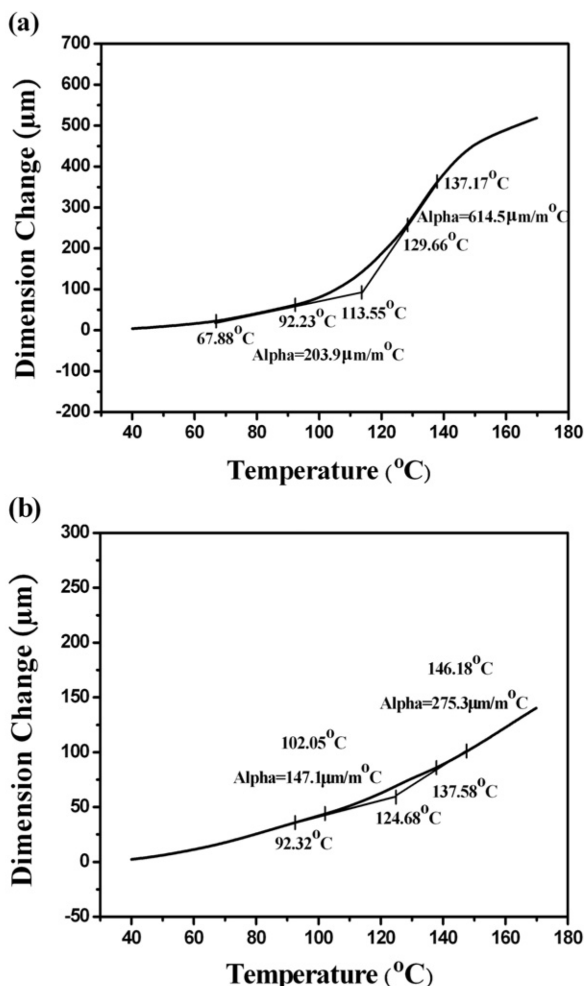

Fig. 8. TMA thermograms of the photoresists. (a) PR54; (b) PR54-MSi20.

Table 3
Hardness, adhesion, and resolution of various photoresists

Sample name	$MSiO_2$ content (wt.%)	Pencil hardness	Adhesion (%)	Resolution (μm)
PR63	0	2H	80	<10
PR63-MSi5	5	3H	100	<10
PR63-MSi10	10	3H	100	<10
PR63-MSi15	15	4H	100	<10
PR63-MSi20	20	5H	100	<10
PR54	0	2H	90	<10
PR54-MSi5	5	3H	100	<10
PR54-MSi10	10	3H	100	<10
PR54-MSi15	15	4H	100	<10
PR54-MSi20	20	5H	100	<10

3.3.2. Adhesion, hardness, and resolution tests

The hardness of the photoresist film coated on glass substrate was examined using the industrial pencil test, whereas the adhesion strength between photoresist and glass was determined by the tape test [20]. For all tested samples, the thickness of the dried coating layer was about 1–2 μm and the tested results are summarized in Table 3. The hardness of both PR63 and PR54 was 2 H, and the value increased with increasing $MSiO_2$ content. A very high hardness of 5 H could be attained when the photoresist contained 20% $MSiO_2$. As to the adhesion strength, all photoresists showed perfect adhesion on the tape test, except samples PR63 and PR54, which were free of $MSiO_2$. It follows

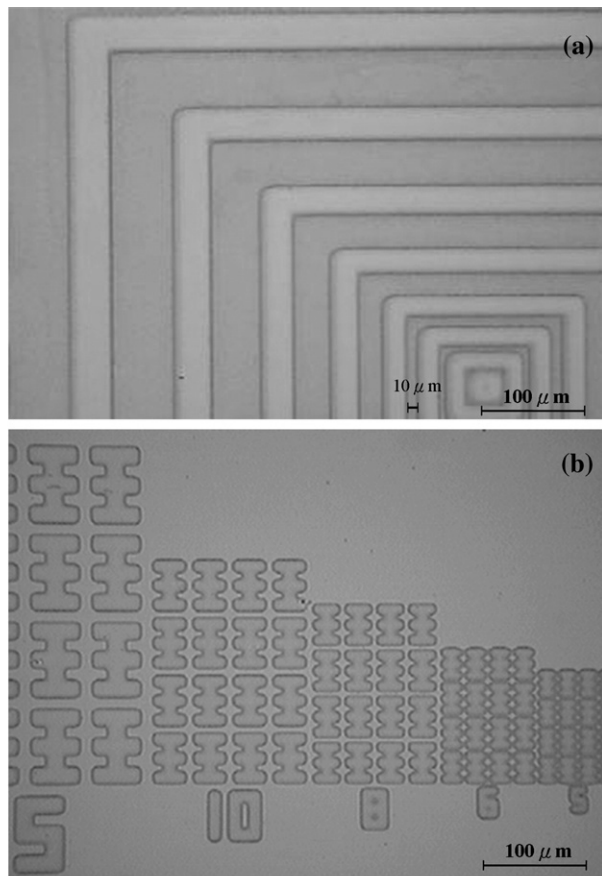

Fig. 9. Optical microscopic image of the patterns formed using photoresist PR54. (a) circuit diagram; (b) resolution test.

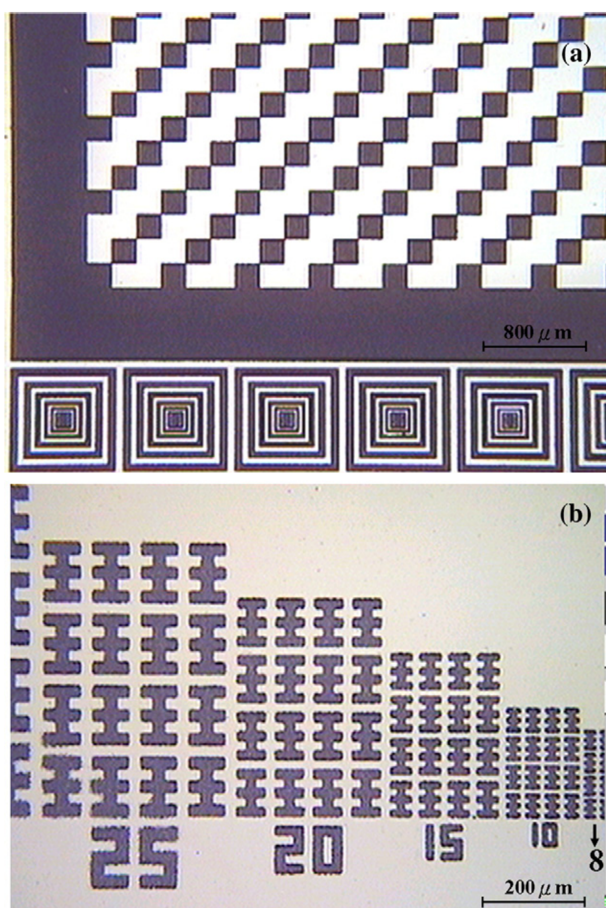

Fig. 10. Optical microscopic image of the patterns formed using photoresist PR54-MSi20. (a) mosaic diagram; (b) resolution test.

that the adhesion strength was also improved by the addition of $MSiO_2$ nanoparticles in the photoresists.

Finally, it is important to know how high the resolution the nano-silica modified photoresist can achieve after a standard exposure-development process, in case that industrial application is targeted. Figs. 9 and 10 show the microscopic images of the developed photoresists, PR54 and PR54-MSi20, respectively. It can be seen that the resolution of PR54 is better than 10 μm. The resolution of PR54-MSi20 also reaches to 10 μm (cf. Fig. 10(b)). In general, incorporation of nano-silica into the photoresist would reduce the developability of the photoresist. However, this problem could be solved by adjustment of the composition of the developer liquid. In the present research, we found that adding a suitable amount of IPA ($IPA/H_2O/Na_2CO_3$ = 3:2:0.02, w/w/w) gives a satisfactory result with a development time of 60 s. The resolution of all other photoresists is within 10 μm, cf. Table 3. In other words, the nano-silica modified photoresists have a resolution meeting the industrial requirement.

4. Conclusions

A nano-silica filled photoresists were synthesized. Their chemical, mechanical and thermal properties have been studied. Several conclusions can be drawn from the experimental observations. The modified $MSiO_2$ nanoparticles, particle size smaller than 10 nm, contain a considerable amount of reactive double bonds (C=C) on their surfaces. They would not only react with the polyfunctional monomers in the photoresist but also increase the compatibility between organic and inorganic components in the photoresist. Incorporation of $MSiO_2$ nanoparticles enhanced the thermal stability of the prepared photoresist: T_d and T_g were found to increase, whereas α_1 and α_2 decrease with increasing $MSiO_2$ content. Nano-silica modified photoresist coated on glass substrate demonstrates a high hardness (5 H) and a strong adhesion (100%) with a resolution reaching 10 μm. For the development process, the optimal weight ratio of $IPN/H_2O/Na_2CO_3$ in developer liquid is found to be 3/2/0.02, with which the nano-silica modified photoresist can be easily developed within 60 s.

Acknowledgements

The authors wish to express their thanks to Prof. Jui-Tang Chen of Ming-Hsin University of Science and Technology for providing photomask for resolution studies.

References

[1] K. Ueda, S. Shioda, H. Nishijima, T. Mukaiyama, S. Mitsuhashi, U.S. Patent No. 6,558,858, 6 May 2003.
[2] M. Sato, M. Iwasaki, F. Shinozaki, K. Inoue, U.S. Patent No. 5,397,678, 14 Mar. 1995.
[3] K. Ueda, S. Shioda, H. Nishijima, T. Mukaiyama, S. Mitsuhashi, U.S. Patent No. 6,432,614, 13 Aug. 2002.
[4] K. Nakamura, S. Sega, U.S. Patent No. 6,582,862, 24 Jun. 2003.
[5] T. Sumino, A. Inoue, U.S. Patent No. 6,680,763, 20 Jan. 2004.
[6] R.W. Sabnis, Displays 20 (1999) 119.
[7] S. O ' Brien, M. Copuroglu, G.M. Grean, Thin Solid Films 515 (2007) 5439.
[8] C. Wu, T. Xu, W. Yang, Eur. Polym. J. 41 (2005) 1901.
[9] D. Blanc, A. Last, J. France, S. Pavan, J.L. Loubet, Thin Solid Films 515 (2006) 942.
[10] C.H. Lin, C.C. Feng, T.Y. Hwang, Eur. Polym. J. 43 (2007) 725.
[11] J. Xu, W. Pang, W. Shi, Thin Solid Films 514 (2006) 69.
[12] C. Wu, T. Xu, M. Gong, W. Yang, Eur. Polym. J. 43 (2007) 1573.
[13] S. Jeong, W.H. Jang, J. Moon, Thin Solid Films 466 (2004) 204.
[14] P. Hajji, L. David, J.F. Gerard, J.P. Pascault, G. Vigier, J. Polym. Sci. Part B: Polym. Phys. 37 (1999) 3172.
[15] G. Bonilla, M. Martinez, A.M. Mendoza, J.M. Widmaier, Eur. Polym. J. 43 (2006) 2977.
[16] J.L. Almaral-Sanchez, E. Rubio, A. Mendoza-Galvan, R. Ramirez-Bon, J. Phys. Chem. Solids 66 (2005) 1660.
[17] M.E.L. Wouters, D.P. Wolfs, M.C. van der Linde, J.H.P. Hovens, A.H.A. Tinnemans, Prog. Org. Coat. 51 (2004) 312.
[18] F.L. Souza, P.R. Bueno, E. Longo, E.R. Leite, Solid State Ionics 166 (2004) 83.
[19] T. Tsushima, M. Kawabata, I. Sumiyoshi, M. Yokoyama, Soc. Inform. Display Digest 25 (1994) 936.
[20] S. Yu, T.K.S. Wong, X. Hu, J. Wei, Microelectron. Eng. 77 (2005) 14.
[21] H.K. Kim, J.G. Kim, J.W. Hong, Polym. Test. 21 (2002) 417.
[22] C.D. Diakoumalos, I. Raptis, A. Tserepi, P. Argitis, Polymer 43 (2002) 1103.
[23] C.R.E. Mansur, M.I.B. Tavares, E.E.C. Monteiro, J. Appl. Polym. Sci. 75 (2000) 495.
[24] S. Krause, J.J. Gormley, N. Roman, J.A. Shetter, W.H. Watanabe, J. Polym. Sci. Part A: Polym. Chem. 3 (1965) 3573.
[25] J. Lee, T. Aoai, S. Kondo, N. Miyagawa, S. Takahara, T. Yamaoka, J. Polym. Sci. Part A: Polym. Chem. 40 (2002) 1858.
[26] K. Baba, S. Hozumi, U.S. Patent No. 6,344,300, 5 Feb. 2002.
[27] Y.Y. Yu, W.C. Chen, Mater. Chem. Phys. 82 (2003) 388.